Structure and thermodynamics of binary liquid mixtures: Universality of the bridge *functional*

Gerhard Kahl,[1] Bernhard Bildstein,[1] and Yaakov Rosenfeld[2,*]
[1]*Institut für Theoretische Physik, Technische Universität Wien, Wiedner Hauptstraße 8-10, A-1040 Wien, Austria*
[2]*H. H. Wills Physics Laboratory, Bristol University, Royal Fort, Tyndall Avenue, Bristol BS8 1TL, United Kingdom*
(Received 5 June 1996)

We investigate in detail a thermodynamically self-consistent method to calculate the thermodynamics and structure of a binary mixture of simple liquids, introduced recently by one of us [Y. Rosenfeld, J. Chem. Phys. **98**, 8126 (1993); Phys. Rev. Lett. **72**, 3831 (1994); J. Phys. Chem. **99**, 2857 (1995); Phys. Rev. E **54**, 2827 (1996)]. This approximation is based on the universality hypothesis of bridge *functionals* and leads to a modified hypernetted-chain-type closure to the Ornstein-Zernike equations. We employ the fundamental-measure bridge functional of hard spheres. The bridge functions are calculated from this functional by inserting the appropriate structure functions of the actual system and of a suitably chosen hard-sphere reference system. An iterative procedure is repeated until numerical self-consistency is obtained. We demonstrate the reliability and wide applicability of this method by comparing numerical results with computer simulation data for a large variety of systems. Finally, we show for the example of the classical inversion problem of liquid state theory that our method can indeed replace computer simulations in more complex procedures without loss of numerical accuracy. [S1063-651X(96)08911-8]

PACS number(s): 64.70.Ja, 61.20.Ne, 61.25.Mv

I. INTRODUCTION

The development of liquid state theory during the past 30 years was characterized by a steady change in predominance between different basic concepts for the determination of the structure and thermodynamics (such as integral equations, simulation methods, and perturbation theories; see, e.g., [1]). By now, the one-component case seems to be settled: these three groups of methods yield, at the respective highest level of sophistication and efficiency, results for the structure and thermodynamics that are equivalent within numerical accuracy [2]. However, the binary case is, from the conceptual point of view, more complex and sometimes still leaves problems unsettled; it therefore represents a stringent test for a recently introduced liquid state theory. In recent years, a diminishing interest in perturbation theories has been observed, leaving thus integral equations and simulation techniques as main concurrents. The problem of thermodynamic inconsistency could not be coped with properly in integral-equation approaches to the binary case. Thermodynamic inconsistency is caused by the approximations done in the derivation of the closure relation from exact thermodynamic relations; as a consequence, different equations of state yield different results for thermodynamic quantities. Simulation techniques do not suffer from this drawback since they are, by definition, thermodynamically self-consistent. During the past years several attempts have been proposed for integral-equation techniques to overcome this consistency problem (such as, e.g., [3–6]). These approaches are mostly based on generalizations of the one-component case, which, however, brings along both conceptual problems (such as, for instance, the restriction to additive reference systems) or numerical problems (a simple equation in one variable now becomes a highly nonlinear set of coupled equations in two or three unknowns where, in addition, it is not always guaranteed that a solution is found).

An approach was introduced recently [7–10] that treats one-component systems and mixtures on equal footing. It starts from the Euler-Lagrange equations, which allow the determination of the one-particle density of an inhomogeneous liquid (''density-profile'' equations) subject to an external field. From these equations we can derive a hypernetted-chain (HNC) type equation for these densities; in those equations the excess free-energy functional F_{ex} enters, which, via functional relations, is closely related to the bridge functional. In previous applications of the modified hypernetted chain (MHNC) or the reference hypernetted chain (RHNC) approximations (e.g., [11]) the unknown bridge functions of a given system were replaced, based on arguments provided by the universality hypothesis [12], by the bridge functions of a suitably chosen hard-sphere (HS) reference system; these functions can be calculated easily within the Percus-Yevick (PY) theory [13] or from the semi-empirical parametrization due to Verlet and Weis [14]. The method imposes universality at the level of the bridge *functional*; similar to the bridge *functions* of a HS system, this *functional* can be calculated very easily for the general case of inhomogeneous hard spheres (involving only fundamental measures) [15] and specialized, as required for our case, to homogeneous hard spheres. This fundamental-measure bridge functional is given in terms of characteristic quantities of the *individual* spheres and involves only integrations over known functions. Furthermore, in this approach the free-energy functional can be optimized by imposing the test-particle (or source-particle) self-consistency, which is realized by the transition from an inhomogeneous system to a homogeneous one if the source of the external potential becomes a particle of the liquid [16]. The Ornstein-Zernike (OZ) equations are then solved for the structure functions of the homogeneous system along with the closure relation

*Permanent address: Nuclear Research Center Negev, P.O. Box 9001, Beer-Sheva 84190, Israel.

where the bridge functions are calculated by means of the above *functional*, assuming that the universality hypothesis is valid. The structure functions obtained are then fed into the bridge functional, yielding an improved set of bridge functions. This procedure is iterated until numerical self-consistency is obtained in a sense that the structure functions of the preceding step differ only marginally from the present step.

The aim of the present paper is twofold. First, we would like to demonstrate the reliability of this approach in direct comparison with computer simulations for mixtures. The systems chosen cover both standard model systems of liquid state theory [HS systems, Coulombic systems, and Lennard-Jones (LJ) mixtures], as well as realistic mixtures, such as binary metal alloys. In particular, attention has been paid to test the reliability of the approach in ''nonstandard'' cases: strongly nonadditive systems with respect to both distance and potential depth. In general, we observe very good agreement between our results and simulation data. Discrepancies are encountered for extreme choices in nonadditivity, where we reach either the limit of the numerical stability of the algorithm or the limits of stability of the system considered. The other aim of this paper is to show that our approximation is *in fact* almost as accurate as computer experiment and is therefore able to replace simulations in more complex algorithms with only little loss in numerical accuracy. To this end we have chosen the problem of inversion in classical liquid state theory: there one tries to extract an effective interatomic pair potential from a given pair structure. An accurate and satisfactory solution of this problem is essential for the interpretation of experimental scattering data [17]. Among others [18–21], a satisfactory approach has been proposed by Levesque *et al.* [22,23]. Their procedure is an iterative predictor-corrector algorithm where the corrector step is represented by a computer simulation. Applications to realistic systems (liquid Ga [24]) demonstrated the power of this approach. The method has been generalized to the binary case [25]: it was found that there the method is as powerful as in the one-component case for ''standard systems.'' The drawbacks are rather caused by numerical inaccuracies in the corrector (simulation) step, in particular, if the concentration of the minority component is small (i.e., $\leqslant 5-10$ %): then the statistical error of the simulation results (for typically 4000–7000 particle ensembles) is too large and leads to an accumulation of errors and, finally, to uncertainties of the results. Smoothing procedures have turned out to bias the results and hence fail as well [26]. In this paper we have therefore replaced in this inversion scheme the simulation step by our method (based on our demonstrated assumption that the present integral-equation results are comparable in accuracy to the computer simulations). This replacement helps us to avoid the above-mentioned problems for small minority concentrations to which integral equations are insensitive.

The paper is organized as follows. In Sec. II we briefly present the basic concept of our approach and present the necessary expressions for the determination of the structure and thermodynamics. Sections II A and II B are concerned with the numerical implementation of the algorithm. Section III provides details about the reference simulations that we have performed and contains a detailed comparison between the results obtained by our density-functional method and data of computer simulations; we furthermore demonstrate by considering the inversion problem that our method can indeed replace computer simulations without loss of numerical accuracy. The paper is concluded by a summary in Sec. IV. Appendixes A and B contain all the necessary expressions that are required to construct the bridge functional and the derivation of the criterion for the reference system parameters.

II. THEORY

A. Basic concept

In an inhomogeneous liquid of N components (and concentrations c_i) where the particles interact via pair potentials $\Phi_{ij}(r)$ and are subject to external potentials $u_i(\mathbf{r})$, $i=1,\ldots,N$, the single-particle densities (or density profiles) $\boldsymbol{\rho}=\{\rho_i(\mathbf{r}), i=1,\ldots,N\}$ are obtained from the Euler-Lagrange equations, i.e., by minimizing the grand potential $\Omega[\boldsymbol{\rho}]$ with respect to the $\rho_i(\mathbf{r})$ [27],

$$\left[\frac{\delta\Omega[\boldsymbol{\rho}]}{\delta\rho_i}\right](\mathbf{r})=0, \quad i=1,\ldots,N. \tag{1}$$

The grand potential is given by

$$\Omega[\boldsymbol{\rho}]=F_{\mathrm{id}}[\boldsymbol{\rho}]+F_{\mathrm{ex}}[\boldsymbol{\rho}]+\sum_i \int d\mathbf{r}\rho_i(\mathbf{r})[u_i(\mathbf{r})-\mu_i], \tag{2}$$

where the μ_i are the chemical potentials and $\boldsymbol{\rho}_0=\{\rho_i=\rho c_i, i=1,\ldots,N\}$ denotes the bulk densities (number densities); ρ is the total (homogeneous) number density.

While the ideal contribution $F_{\mathrm{id}}[\boldsymbol{\rho}]$ in Eq. (2) can be given by the exact relation

$$F_{\mathrm{id}}[\boldsymbol{\rho}]=k_BT\sum_i \int d\mathbf{r}\rho_i(\mathbf{r})\{\ln[\rho_i(\mathbf{r})\lambda_i]-1\} \tag{3}$$

(the λ_i are the de Broglie wavelengths), the crucial quantity within this framework remains the excess part of the free energy $F_{\mathrm{ex}}[\boldsymbol{\rho}]$, which stems from the interaction of the particles. A hierarchy of the direct correlation functions $c^{(n),\mathrm{FD}}_{1,\ldots,n}[\boldsymbol{\rho}](\mathbf{r}_1,\ldots,\mathbf{r}_n)$ is derived from $F_{\mathrm{ex}}[\boldsymbol{\rho}]$ via functional derivatives (FD) with respect to the one-particle densities:

$$k_BTc_i^{(1),\mathrm{FD}}[\boldsymbol{\rho}](\mathbf{r}_1)=-\mu_{i,\mathrm{ex}}[\boldsymbol{\rho}](\mathbf{r}_1)=-\left[\frac{\delta F_{\mathrm{ex}}[\boldsymbol{\rho}]}{\delta\rho_i}\right](\mathbf{r}_1), \tag{4}$$

$$k_BTc_{ij}^{(2),\mathrm{FD}}[\boldsymbol{\rho}](\mathbf{r}_1,\mathbf{r}_2)=-\left[\frac{\delta^2 F_{\mathrm{ex}}[\boldsymbol{\rho}]}{\delta\rho_i\delta\rho_j}\right](\mathbf{r}_1,\mathbf{r}_2). \tag{5}$$

The $\mu_{i,\mathrm{ex}}$ are the excess chemical potential functionals and k_B is the Boltzmann constant. We start from a (formally exact) functional Taylor expansion of $F_{\mathrm{ex}}[\boldsymbol{\rho}]$ around the uniform fluid limit in terms of the $\Delta\rho_i(\mathbf{r})=[\rho_i(\mathbf{r})-\rho_{i,0}]$:

$$F_{\mathrm{ex}}[\boldsymbol{\rho}]=F_{\mathrm{ex}}^{(2)}[\boldsymbol{\rho}_0;\boldsymbol{\rho}]+F_{\mathrm{ex}}^{B}[\boldsymbol{\rho}_0;\boldsymbol{\rho}]. \tag{6}$$

$F_{ex}^{(2)}[\boldsymbol{\rho}_0;\boldsymbol{\rho}]$ is given by

$$F_{ex}^{(2)}[\boldsymbol{\rho}_0;\boldsymbol{\rho}]=F_{ex}[\boldsymbol{\rho}_0]+\sum_i \mu_{i,ex}[\boldsymbol{\rho}_0]\int d\mathbf{r}\,\Delta\rho_i(\mathbf{r}) - \frac{k_BT}{2}\sum_{i,j}\int\int d\mathbf{r}\,d\mathbf{r}'\,c_{ij}^{(2),FD}[\boldsymbol{\rho}_0](|\mathbf{r}-\mathbf{r}'|) \times\Delta\rho_i(\mathbf{r})\Delta\rho_j(\mathbf{r}'). \quad (7)$$

$c_{ij}^{(2),FD}[\boldsymbol{\rho}_0](|\mathbf{r}-\mathbf{r}'|)$ is the direct correlation function of the homogeneous (bulk) system. In the above Taylor expansion the exact terms up to order 2 are subsumed in $F_{ex}^{(2)}[\boldsymbol{\rho}]$ and the subsequent term $F_{ex}^{B}[\boldsymbol{\rho}]$ contains all contributions of order three and higher. It is related to the bridge functional $B_i[\boldsymbol{\rho}_0;\boldsymbol{\rho}](\mathbf{r})$ via

$$B_i[\boldsymbol{\rho}_0;\boldsymbol{\rho}](\mathbf{r})=\frac{1}{k_BT}\left[\frac{\delta F_{ex}^{B}[\boldsymbol{\rho}_0;\boldsymbol{\rho}]}{\delta\rho_i}\right](\mathbf{r}). \quad (8)$$

It can now be shown for a fluid in contact with a reservoir bulk fluid of density $\boldsymbol{\rho}_0$ that Eq. (1), which determines the density profiles, can be cast in the (HNC type) form [7–10]

$$\ln[g_i(\mathbf{r})]=-\frac{1}{k_BT}u_i(\mathbf{r})+B_i[\boldsymbol{\rho}_0;\boldsymbol{\rho}](\mathbf{r}) + \sum_j \rho_{j,0}\int d\mathbf{r}'\,c_{ij}^{(2),FD}[\boldsymbol{\rho}_0](|\mathbf{r}-\mathbf{r}'|)[g_j(\mathbf{r}')-1], \quad (9)$$

introducing $g_i(\mathbf{r})=\rho_i(\mathbf{r})/\rho_{i,0}$; the bridge functional (8) turns out to be given by

$$B_i[\boldsymbol{\rho}_0;\boldsymbol{\rho}](\mathbf{r})=\frac{1}{k_BT}\{\mu_{i,ex}[\boldsymbol{\rho}](\mathbf{r})-\mu_{i,ex}[\boldsymbol{\rho}_0]\} + \sum_j \rho_{j,0}\int d\mathbf{r}'\,c_{ij}^{(2),FD}[\boldsymbol{\rho}_0](|\mathbf{r}-\mathbf{r}'|) \times[g_j(\mathbf{r}')-1]. \quad (10)$$

Following an old idea of Percus [16], we recover within this formalism the properties of the *homogeneous* liquid from the *inhomogeneous* liquid by interpreting the source of the external fields $[u_i(\mathbf{r})]$ as a particle (t) of the liquid itself, situated at the origin and interacting with the other particles via $u_i(\mathbf{r})=\Phi_{ti}(\mathbf{r})$; the formalism is called the source or test particle method and will help us in the following to describe the properties of the homogeneous system. The $g_i(\mathbf{r})$ introduced above now become the pair distribution functions (PDFs) $g_{ti}(r)$ and the density-profile equations (9) reduce to

$$\ln[g_{ti}(r)]=-\frac{1}{k_BT}\Phi_{ti}(r)+\overline{b_{ti}}(r) + \sum_j \rho_{j,0}\int d\mathbf{r}'\,c_{ji}^{(2),FD}(|\mathbf{r}-\mathbf{r}'|) \times h_{tj}(r'). \quad (11)$$

$h_{ti}(r)[=g_{ti}(r)-1]$ and the $\overline{b_{ti}}(r)$ stand for the symmetrized bridge functions

$$\overline{b_{ti}}(r)=\frac{c_ib_{ti}(r)+c_tb_{it}(r)}{c_t+c_i}, \quad (12)$$

which have to be introduced in this form in order to preserve symmetry in the indices $[b_{ti}(r)=b_{it}(r)]$ in this generalization of the test particle formalism to the binary case.

For a given $F_{ex}[\boldsymbol{\rho}]$ the density-profile (DP) equations (9) and (10) can now be solved and yield the PDFs $g_{ij}^{DP}(r)$. On the other hand, the direct correlation functions $c_{ij}^{(2),FD}(r)$ [obtained via functional derivative from $F_{ex}[\boldsymbol{\rho}]$ via (5)] fulfill, along with the PDFs $g_{ij}^{OZ}(r)$, the Ornstein-Zernike relations

$$h_{ti}^{OZ}(r)=c_{ti}^{(2),FD}(r)+\sum_j \rho_{j,0}\int d\mathbf{r}'\,c_{ji}^{(2),FD}(|\mathbf{r}-\mathbf{r}'|)h_{tj}^{OZ}(r'). \quad (13)$$

Up to now no approximations have been made.

If we were to know the *exact* $F_{ex}[\boldsymbol{\rho}]$ then the two sets of PDFs (labeled OZ and DP) would be equal (i.e., consistent); this consistency is referred to as the test particle self-consistency. However, since for realistic applications approximations have to be admitted to construct the functional of the excess free energy, this consistency will, in general, be violated, i.e., the $g_{ij}^{DP}(r)$ will differ from the $g_{ij}^{OZ}(r)$. Nevertheless, given some model for the bridge functional (and hence for $F_{ex}[\boldsymbol{\rho}]$), this functional can be optimized by imposing self-consistency, i.e., by requiring that Eqs. (11) *and* (13) are fulfilled.

Several years ago the universality hypothesis of the bridge functions [12] introduced a breakthrough in the actual implementation of the MHNC and RHNC methods: this hypothesis ''allows'' the bridge functions of a given system to be replaced, within a good accuracy, by the bridge functions of a suitably chosen HS reference system. In the present method this hypothesis is generalized to the level of *functionals*: to this end the contribution $F_{ex}^{(B)}[\boldsymbol{\rho}]$ in (6) is replaced by a functional $F_{ex}^{(B),ref}[\boldsymbol{\rho}]$ of a suitably chosen reference system, which generates the bridge functional of the reference system, $B_i^{ref}[\boldsymbol{\rho}_0;\mathbf{g}](\mathbf{r})$, similar to (8) and

$$b_{ti}(r)=B_i^{ref}[\boldsymbol{\rho}_0;\mathbf{g}](\mathbf{r}), \quad (14)$$

where $\mathbf{g}$ stands for the set of PDFs $g_{ti}(r)$. Similar to (10), $B_i^{ref}[\boldsymbol{\rho}_0;\mathbf{g}](\mathbf{r})$ is found to be given by [7–10]

$$B_i^{ref}[\boldsymbol{\rho}_0;\mathbf{g}](\mathbf{r})=\frac{1}{k_BT}\{\mu_{i,ex}^{ref}[\boldsymbol{\rho}](\mathbf{r})-\mu_{i,ex}^{ref}[\boldsymbol{\rho}_0]\} + \sum_j \rho_{j,0}\int d\mathbf{r}'\,c_{ij}^{(2),FD,ref}[\boldsymbol{\rho}_0](|\mathbf{r}-\mathbf{r}'|) \times[g_j(\mathbf{r}')-1]. \quad (15)$$

Note that $B_i^{ref}[\boldsymbol{\rho}_0;\mathbf{g}](\mathbf{r})$ also contains the structure functions $g_{ti}(r)$ of the considered system.

Two questions now remain open: (i) what reference system is chosen to provide the reference bridge functional and (ii) how do we determine the parameters of this reference system? The most natural choice for a reference system in liquid state theories for simple liquids are hard spheres (see,

e.g., Refs. [1,28] and other papers cited therein). In addition, as it has been shown recently by one of us [15], it is possible to construct an excess free-energy functional $F_{\rm ex}^{\rm HS}[\boldsymbol{\rho}]$ [and hence $B_i^{\rm HS}[\boldsymbol{\rho}_0;\mathbf{g}](\mathbf{r})$] for a binary system of additive HS compatible with the analytic PY solution of the OZ equations [29]. (There are indications that also for other model systems for which analytic solutions exist in liquid state theory, such as HS Yukawa systems, such a functional might be constructed, however, with a much larger formal effort [30,31]). This HS free-energy functional will be used as the reference free-energy functional $F_{\rm ex}^{\rm ref}[\boldsymbol{\rho}]$. Details about the construction of this functional and the resulting expressions for the bridge functional $B_i^{\rm ref}[\boldsymbol{\rho}_0;\mathbf{g}](\mathbf{r})$ are given in [7,8,15] (see also Appendix A). The second question of how the parameters of this reference system are determined can be answered following similar lines as in the MHNC-RHNC approximations: for the bridge *function* based methods, Lado [11,32,33] has derived criteria for the determination of the packing fraction of the HS reference system. As outlined in more detail in Appendix B, we can generalize these criteria to our bridge *functional* based method and arrive at the following equations, which fix the parameters of the reference system:

$$\sum_{i,j} \rho_{i,0}\rho_{j,0} \int d\mathbf{r}[g_{ij}(r)-g_{ij}^{\rm ref}(r)]\delta\overline{b_{ij}^{\rm ref}}(\mathbf{g};r)=0. \quad (16)$$

A similar and more easy to handle, though less accurate, criterion

$$\sum_{i,j} \rho_{i,0}\rho_{j,0} \int d\mathbf{r}[g_{ij}(r)-g_{ij}^{\rm ref}(r)]\overline{b_{ij}^{\rm ref}}(\mathbf{g};r)=0 \quad (17)$$

has also been tested in this contribution. For the case of a HS reference system, Eq. (16) becomes

$$\sum_{i,j} \rho_{i,0}\rho_{j,0} \int d\mathbf{r}[g_{ij}(r)-g_{ij}^{\rm ref}(r)]\frac{\partial\overline{b_{ij}^{\rm ref}}(\mathbf{g};r)}{\partial d_{kk}}=0, \quad k=1,2, \quad (18)$$

i.e., a set of two coupled nonlinear equations in two variables (d_{11} and d_{22}).

Once the above problem has been solved it is easy to extract all further structural information. We can therefore now proceed to the determination of the thermodynamic properties. Pressure and internal energy follow from the standard relations [1]. Like in the implementation of the universality of the bridge functions, we can replace the Lado criterion by choosing the reference parameters such that *thermodynamic consistency* is obeyed. But this does not allow the local determination of the free energy and chemical potentials, which have to be obtained by integration along a thermodynamic path *after* solving the integral equations for the set of points in the (ρ,T) plane.

B. Numerical implementation

The numerical realization is based on an efficient algorithm [34] implementing an algorithm proposed by Gillan to solve integral equations in liquid state physics [35]. In general, we start from the HNC solution, i.e., from the closure

$$g_{ij}(r)=\exp[-\beta\Phi_{ij}(r)+h_{ij}(r)-c_{ij}(r)]. \quad (19)$$

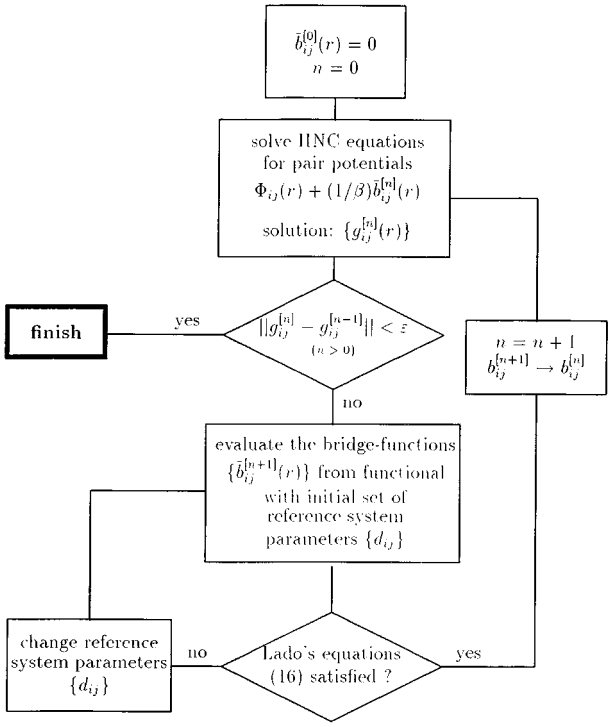

FIG. 1. Flow chart of the numerical implementation of the proposed algorithm.

This solution is the starting point of an iterative process.

(i) The structure functions $g_{ij}^{\rm HNC}(r)=g_{ij}^{[0]}(r)$ (and the other correlation functions) are fed into the bridge functional (15) yielding the bridge functions $b_{ti}(r)$ via (14); for the HS reference system some set of diameters d_{11} and d_{22} is assumed (actually, in a first guess, we pick some value for the packing fraction η and the ratio of the diameters is fixed to some value characteristic for the system as, e.g., the positions of the minima in the potentials).

(ii) The OZ equations are solved along with the closure relations

$$g_{ij}(r)=\exp[-\beta\Phi_{ij}(r)+h_{ij}(r)-c_{ij}(r)+\overline{b_{ij}}(r)], \quad (20)$$

with the bridge functions taken from (14).

(iii) The expressions in (16) [or (17)] are evaluated for a given set of parameters d_{11} and d_{22}: if the set of coupled equations are fulfilled then we proceed with the next step (iv); if the equations are not fulfilled, then the parameters are modified and we go back to the preceding step (ii); again this loop is realized in a first, coarse search for η and assuming a fixed ratio of diameters. In a refinement step we introduce the full dependence on the *two* parameters.

(iv) The bridge functions that we have obtained in this way are fed into the closure relation (20) and we restart at step (ii).

The whole bridge cycle is depicted in a flow chart in Fig. 1.

In practice all results presented here have been obtained for ten bridge cycles (although in some cases a smaller number would have been sufficient). Furthermore, we found that the full Lado criterion (16) leads to more reliable results than

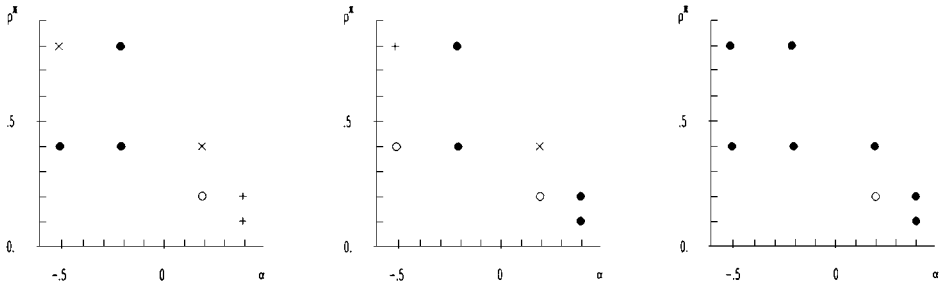

FIG. 2. Schematic representation of the nonadditive HS systems investigated in this study. The three different figures correspond to three different c_1 values: (a) $c_1=0.1$, (b) $c_2=0.25$, and (c) $c_1=0.4$. Every symbol in the (α,ρ^*) plane represents one system, forming, along with the corresponding c_1 value, the triplet of (c_1,α,ρ^*) necessary to characterize the system. Symbols denote the following: ●, successful convergence of the algorithm; ○, convergence of the algorithm, but with unphysical parameters for the reference system; +, convergence possible with numerical tricks; and ×, no convergence possible.

(17). Also introducing the full dependence on both parameters d_{11} and d_{22} instead of using only one parameter η (with fixed d_{11}/d_{22}) leads to improved results, even though from the mathematical or numerical point of view, the latter criterion would provide a faster solution of the problem.

III. RESULTS

A. Comparison with computer simulations

The structure data obtained by our method have been compared to simulation results. Both for HS and Coulombic systems we took data from the literature: in the first case we used the extensive study of (nonadditive) hard spheres performed recently by means of Monte Carlo (MC) simulation by Jung *et al.* [36,37], while the MC results for the Coulombic system stem from DeWitt *et al.* [38]. For details about those simulations we refer the readers to the respective publications.

For the LJ mixtures and the binary metallic alloys our data were complemented by results obtained from standard microcanonical molecular-dynamics (MD) simulations; the equations of motion are integrated with a fourth-order Gear ''predictor-corrector'' algorithm. The ensemble size was, in all cases, chosen to be 4000 particles; results represent ensemble averages over 20 000 time steps. Details about the simulations used in the inversion problem are given in Sec. III B.

1. Hard spheres

The most simple binary model systems are mixtures of hard spheres. The fact that the analytic PY solution predicts [39] that no phase separation is possible within this framework has made those systems less attractive over a long period. Only recently, studies (e.g., by means of very accurate integral-equation techniques and simulations) have revealed, despite the simplicity of the interatomic potential, a large variety of phase separating behavior of both additive and nonadditive hard spheres. In particular, during the past several years special interest has been devoted to interesting phenomena encountered, e.g., in additive but highly asymmetric mixtures [8,40] or nonadditive mixtures (see [6,36,37,41,42] and references cited therein).

Our investigations of the structure of binary HS systems follows closely a recent MC study [36] of symmetric nonadditive hard spheres [i.e., of a mixture of equally sized spheres $d_{11}=d_{22}$ and $d_{12}=\frac{1}{2}(d_{11}+d_{22})(1+\alpha)$]. The systems are furthermore characterized by the concentration c_1 of species 1 and a reduced dimensionless density $\rho^*=\rho(c_1d_{11}^3+c_2d_{22}^3)$. The packing fraction η is then given by $\eta=(\pi/6)\rho^*$. Characterizing the systems by triplets (c_1,α,ρ^*), we have studied on the whole 25 mixtures; the parameters of 24 systems are depicted schematically in Fig. 2 for fixed c_1 values in a (α,ρ^*) plane. In addition, we have considered the system (0.5, 0.5, 0.15). As indicated in the caption of Fig. 2, these graphs give also some information about the quality of the results as such and in comparison to computer simulations. In Fig. 3 we have depicted the PDFs of four selected systems along with MC data [36].

At the practical application of our proposed method we were faced in principle with two problems: (i) whether the limits of the numerical stability of the algorithm correspond to the limits of stability of the system investigated; (ii) for several systems, convergence of the algorithm (with reasonable results for the PDFs and good agreement with simulation data) was obtained, however, with unphysical parameters of the reference system. The phase diagram of nonadditive hard spheres was investigated thoroughly and in principle we knew about the phase limits from those previous investigations [6,36,37,42]; however, the exact limits of stability are very sensitive to the numerical method used. In general, we found that convergence was rather difficult to obtain as we approached the phase stability regime predicted by one or the other method. Among the 25 systems treated in this study and chosen more or less at random (cf. Fig. 2), for only three mixtures no convergence could be obtained at all. As can be seen in Fig. 3, these systems are all close to the phase separating region. For three of the systems numerical convergence could be obtained; however, the reference system parameters were unphysical. Again, those systems were close to the stability region. For all other systems (i.e., the large majority) we found results that gave very satisfactory agreement with simulation data (for a few cases additional numerical tricks had to be applied to guarantee convergence).

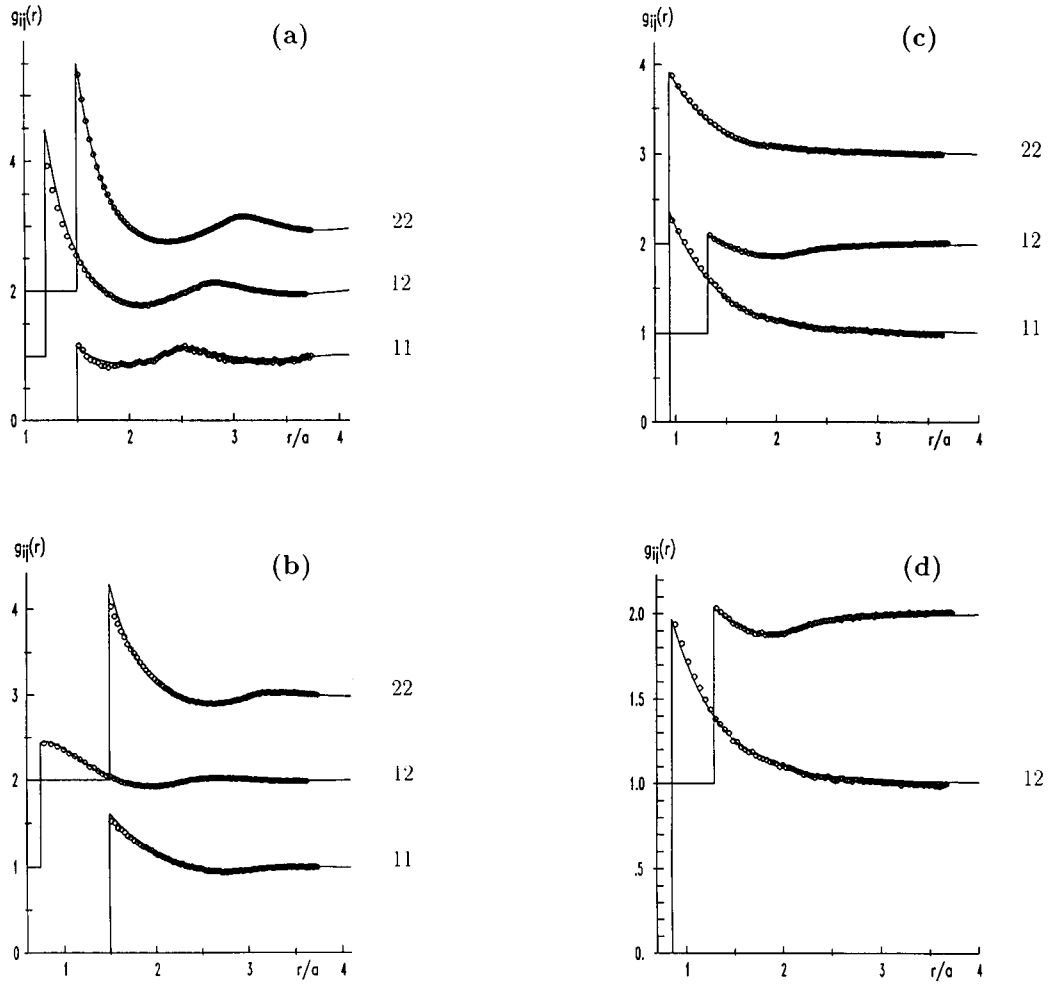

FIG. 3. Partial PDFs $g_{ij}(r)$ (as labeled) as functions of r for binary symmetric nonadditive HS systems considered in our study for the following (c_1,α,ρ^*) triplets as functions of r/a $(a^3=[(3/4\pi)(1/\rho^*)])$: (a) (0.1,−0.2,0.8), (b) (0.4,−0.5,0.8), (c) (0.4, 0.4, 0.2), and (d) (0.5, 0.5, 0.15). Symbols denote the following: ○, MC results [36]; line, present study.

In the following we try to summarize the influence of the three system parameters c_1, α, and ρ^* on the quality of our results. The most critical parameter turned out to be the density ρ^*: a high density leads, in general, to a slow convergence, unsatisfactory results, or sometimes even to no convergence at all. In addition, an influence of the concentration can be observed: if we follow, e.g., the sequence of systems defined by $(c_1,0.4,0.2)$ with $c_1=0.1$, 0.25, and 0.4, then we see that for the first two systems no convergence could be obtained, while we found very good agreement for the $c_1=0.4$ case [see also Fig. 3(c)]. From this we can conclude that a strong nonadditivity can be compensated more easily for a more equilibrated concentration distribution of the particles in the mixture: in general, one observes better results for those cases where the differences in the concentrations are not too large. Finally, nonadditivity as such (if it does not reach extreme values) turns out to be no crucial parameter for the convergence of the algorithm. Finally, we want to note that we could not find correlations between the packing fraction of the reference system η_{ref} and the effective packing fraction of the nonadditive HS system (defined, e.g., as $\eta_{\mathrm{eff}}=(\pi/6)\rho^*[1+(1+\alpha)^3]$; cf. [43]).

Figure 3 shows the PDFs obtained by our method in comparison with MC data [36] for four selected systems: Fig. 3(a) displays results for a system where convergence was very slow, while the slow decay of the PDFs as functions of the distance r in Fig. 3(d) indicates a near phase transition.

2. Coulombic system

In Fig. 4 we present results of the PDFs that we have calculated for a binary ionic mixture, i.e., of a system of point ions in a uniform neutralizing background in comparison with MC data [38]. We consider several such systems where the charges are given by $Z_1=1$ and $Z_2=5$ and a parameter Γ_1, with $\Gamma_1=\Gamma Z_1^{5/3}\sqrt[3]{(c_1Z_1+c_2Z_2)}$. $\Gamma=e^2/(ak_BT)$ is the usual coupling parameter and a is the Wigner-Seitz radius $(1/\rho=4\pi a^3/3)$. Agreement is very satisfactory; this also holds for the (reduced dimensionless) potential energy $U^*=U/Nk_BT$, which we have compiled, along with the parameters of the systems investigated, in Table I.

3. Lennard-Jones systems

The most simple (continuous) model systems with an attractive potential tail are LJ systems. We use the standard

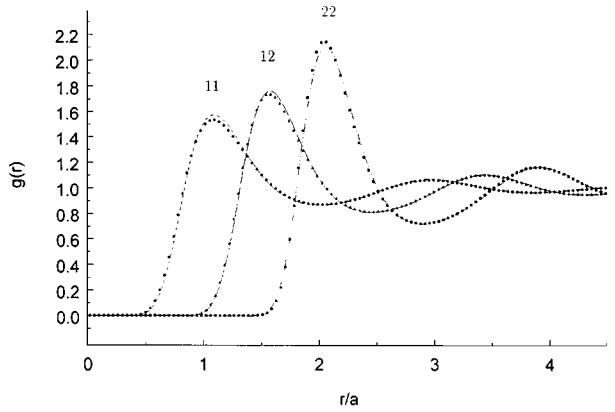

FIG. 4. Partial PDFs $g_{ij}(r)$ (as labeled) as functions of r (in units of the Wigner-Seitz radius a of the equimolar ($c_1=c_2=0.5$) binary Coulombic system considered in our study (for system parameters cf. the text and Table I): ●, MC results [38]; line, present study.

parametrization (with the distance parameters σ_{ij} and the potential parameters $\varepsilon_{ij}^*=\varepsilon_{ij}/k_BT$) and the usual expressions for the interatomic potentials

$$\Phi_{ij}^*(r)=\beta\Phi_{ij}(r)=4\varepsilon_{ij}\left[\left(\frac{\sigma_{ij}}{r}\right)^{12}-\left(\frac{\sigma_{ij}}{r}\right)^{6}\right]. \qquad (21)$$

The parameters σ_{ij} and ε_{ij}, $i,j=1,2$, of the systems investigated in this study have been taken from an Ar-Kr mixture used in a MC study [44] and reused recently in an application of a binary RHNC version [5]. Based on this (additive) model system we have introduced nonadditivity both with respect to distance and energy via

$$\sigma_{ij}=\tfrac{1}{2}(\sigma_{ii}+\sigma_{jj})(1+\alpha), \quad \varepsilon_{ij}=\xi\sqrt{\varepsilon_{ii}\varepsilon_{jj}}. \qquad (22)$$

The parameters α and ξ used in this study are compiled in Table II. As explained in the caption, the table also contains information where problems (concerning either the numerical convergence or discrepancies with computer simulation data) were encountered (cf. also discussion below).

Except for the systems characterized by large nonadditivity parameters ($\alpha=-0.2$ or $+0.1$ and/or $\xi=0.9$ or 1.1), we obtained very satisfactory agreement with MD data. Among all these systems considered in this study we have chosen a few with a high degree of nonadditivity and have depicted them in Fig. 5: Fig. 5(a) shows the perfect agreement that is encountered for most of the systems investigated. This peculiar system is characterized by the (ξ,α) pair (0.9, 0.0), i.e., the mixture is additive with respect to the distances and nonadditive with respect to the potential depth. Figures 5(b) and 5(c) show results for the systems (1.1, −0.15) and (1.1, 0.10), i.e., for rather strongly nonadditive mixtures. Even though slight differences between the numerical and the simulation data are observed, these figures demonstrate, nevertheless, the wide applicability of our proposed method: for the first system, the characteristic wiggles in $g_{11}(r)$ around 7 Å are reproduced very nicely and for the other system we still obtain very good agreement even though the peak heights of the three partial PDFs have become already rather high, i.e., the system is quite dense.

TABLE I. Parameters for the binary Coulombic systems considered in this study and results for the reduced dimensionless potential energy $U^*=U/(Nk_BT)$ in comparison with simulation (MC) and HNC results. η is the packing fraction of the HS reference system.

Z_1	Z_2	Γ_1	c_2	U^*_{MC} [a]	U^*	U^*_{HNC}	η
1	5	10	0.05	−14.02753 ± 0.00015	−14.0081	−13.929	0.292
1	5	10	0.10	−20.05840 ± 0.00017	−20.0301	−19.926	0.330
1	5	10	0.20	−32.12399 ± 0.00023	−32.0974	−31.924	0.382
1	5	10	0.50	−68.33913 ± 0.00032	−68.3609	−67.940	0.451

[a]Reference [38].

TABLE II. Parameters of the LJ systems (Ar-Kr mixture with parameters taken from [44]) investigated in this study. For all systems the following parameters have been chosen: $\rho=0.01834$ Å^{-3}, $T=115.8$ K, and $c_{\mathrm{Ar}}=c_{\mathrm{Kr}}=0.5$; $\sigma_{\mathrm{Ar}}=3.405$ Å, $\sigma_{\mathrm{Kr}}=3.633$ Å, $\varepsilon^*_{\mathrm{Ar}}=1.0345$, and $\varepsilon^*_{\mathrm{Kr}}=1.442$. The Ar-Kr parameters are defined via $\sigma_{\mathrm{Ar\,Kr}}=\frac{1}{2}(\sigma_{\mathrm{Ar}}+\sigma_{\mathrm{Kr}})(1+\alpha)$ and $\varepsilon_{\mathrm{Ar\,Kr}}=\xi(\varepsilon_{\mathrm{Ar}}\varepsilon_{\mathrm{Kr}})^{1/2}$. For systems marked by ○ or ● no numerical problems were encountered and agreement with MD data was very satisfactory (cf. the text and figures); ● indicates those systems for which the PDFs are depicted in Fig. 5. For systems marked by × no numerical convergence of the procedure could be obtained and for the system marked by + numerical convergence was obtained, but agreement with simulation data was found to be unsatisfactory. The last line lists the packing fraction η of the HS reference system (the values depend only weakly on ξ).

ξ	α						
	−0.20	−0.15	−0.10	−0.05	0.0	0.0	0.10
0.9	×	○	○	○	●	○	×
1.0	×	○	○	○	○	○	×
1.1	+	●	○	○	○	○	●
	η=0.28	η=0.28	η=0.34	η=0.39	η=0.43	η=0.45	η=0.46

4. Binary alloys

As a final class of model systems we have chosen binary alloys, which, in contrast to LJ mixtures, are characterized by *long-ranged* attractive oscillating pair potentials. For simplicity we have chosen in this study a binary alkali alloy K_cCs_{1-c}, varying c over the entire concentration range and considering three different temperatures. This system has been object to a previous experimental [45] and therefore, as one of the rare binary systems for which extensive neutron-scattering experiments have been performed, to several theoretical investigations [4,46,47]. Similar integral-equation studies have been performed on other alkali alloys [48]. The interatomic potentials are based on pseudopotential theory, using a simple Ashcroft ''empty-core'' pseudopotential [49] and the Ichimaru-Utsumi parametrization for the exchange-correlation corrections [50]. The logarithmic singularity in the Lindhard function is known to be responsible for the long-ranged oscillations in the potentials [51]. The number

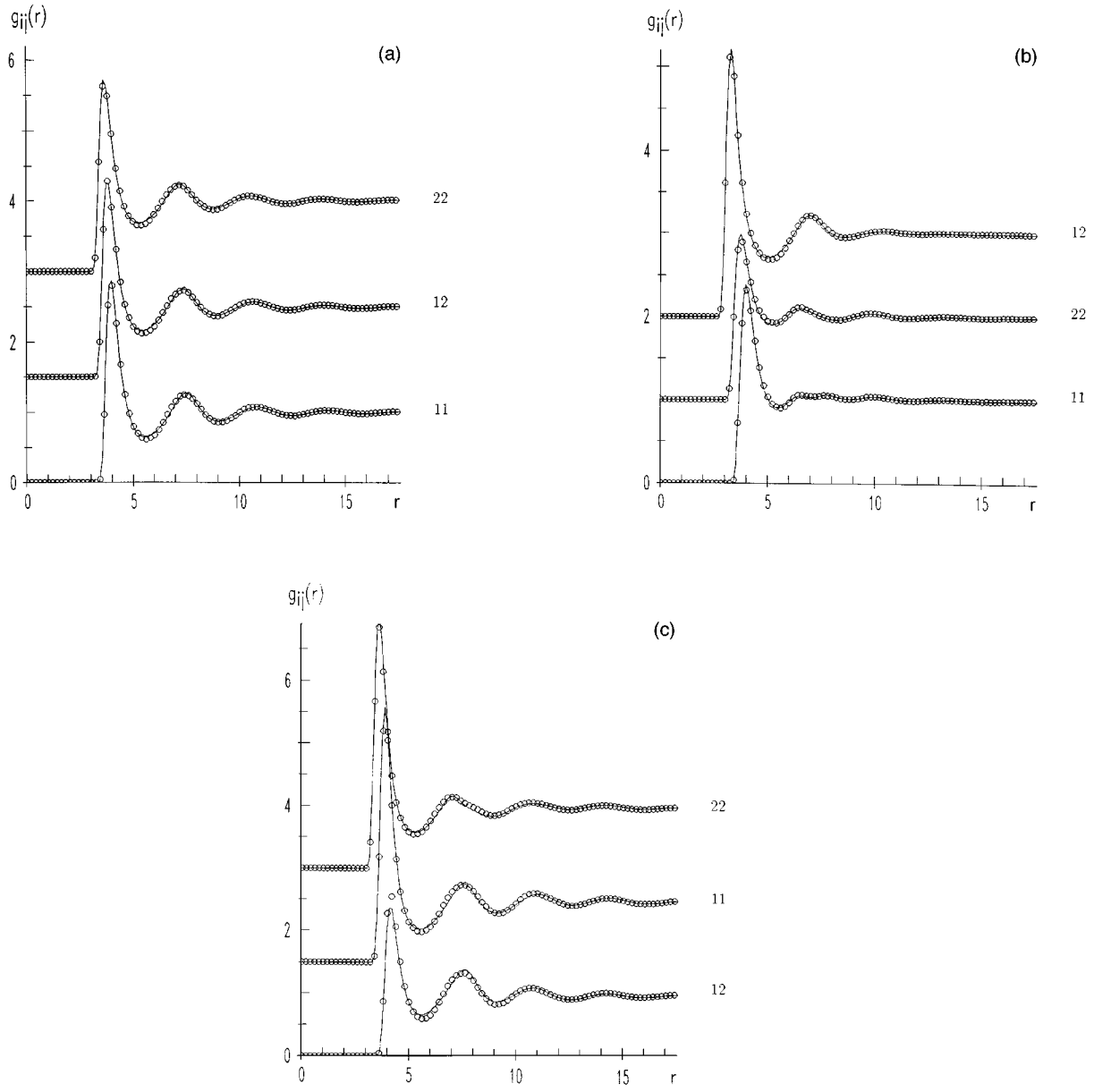

FIG. 5. Partial PDFs $g_{ij}(r)$ (as labeled) as functions of r (in angstroms) for the three LJ systems (Ar-Kr) considered in our study (for system parameters cf. the caption of Table II) with the following (ξ,α) parameters: (a) (0.9,0.0), (b) (1.1,−0.15), and (c) (1.1,0.10). Symbols denote the following: ○, MD data; lines, present study.

densities of the systems have been taken from [52]; the other parameters characterizing the model for the systems are compiled in Table III. We have compared data obtained by our proposed method with MD results and HMSA data [53] [i.e., a parametrized integral-equation method, with a closure interpolating between HNC and soft MSA (SMSA)]; in the latter case thermodynamic self-consistency was obtained by means of one adjustable mixing parameter and requiring equality for the compressibility obtained via the virial and the compressibility route. In the previous HMSA study on this system [4] it was found that for lower temperatures (in our case, at 373 K) self-consistency could not be obtained for the allowed range of the mixing parameter; however, for higher temperatures equality between the two routes could be fulfilled and led, in comparison to simulation data, to a net improvement over simple, unparametrized integral-equation approaches, such as the SMSA or the HNC approximation.

In Fig. 6 we present results obtained by the method presented here and compare them with simulation results. Since for all systems agreement turned out to be very satisfactory (i.e., within numerical accuracy) we restrict ourselves to two typical examples, which are marked in Table III. In contrast to the HMSA integral-equation approach, we were able to obtain with our method self-consistency for *all* systems, i.e., even for low temperatures. In a direct comparison at higher temperatures, differences between the thermodynamically self-consistent HMSA data and the present results turn out to be very small.

TABLE III. System parameters of the K_cCs_{1-c} alloys investigated in this study. The core radii r_c of the Ashcroft ''empty-core'' pseudopotential are chosen to be $r_c=1.2012$ Å (K) and $r_c=1.4393$ Å (Cs) [51]; the listed number densities are obtained from data in [52] by linear interpolation of the atomic volumes. η is the packing fraction of the HS reference system. Systems marked by * are depicted in Fig. 6.

c_K	T (K)	ρ (Å^{-3})	η
0.2	373	0.00876	0.45
0.4	373	0.00949	0.45
0.6	373	0.01034	0.45
0.7	373	0.01083	0.45
0.8*	373	0.01137	0.45
0.4*	773	0.00833	0.32
0.7	973	0.00889	0.28

5. Bridge functions

Similar to a previous study on the one-component case [10], we have also studied the r dependence of the bridge functions obtained from our method. They are displayed in a logarithmic plot in Fig. 7 for two binary ionic mixtures [Fig. 7(a)] and for two metallic alloys [Fig. 7(b)]; for the LJ systems we obtain results similar to those for the binary alloys. The crucial parameter to characterize the behavior is the packing fraction η of the reference system; for the cases displayed in Fig. 7 the corresponding values are indicated in the caption. We also note, despite similar η values, characteristic differences in the range of the bridge functions between ionic and strongly repulsive systems: while in the first case the $b_{ij}(r)$ decay rapidly as functions of r, the oscillations of the bridge functions of the binary alloys extend over a large r range (the distance is measured in Wigner-Seitz units a). In both cases the decay turns out to be faster as the packing fraction decreases. We also note the characteristic oscillations that are already observed from $r\sim 2a$ onward; they are similar to the oscillations encountered for the PDFs where they are caused by the distribution of the poles of the Laplace transform of the PDFs. This has been observed by Martynov [54] and discussed in detail by Evans and co-workers [55] (for the binary case see also [56]).

B. Application: The binary inversion problem

A few years ago, Levesque *et al.* [22,23] proposed an iterative procedure for the solution of the ''inversion problem'' of classical liquid state theory, i.e., the determination of an effective pair interaction from the pair structure. Initial attempts to solve this problem date back to the 1960s [18] and were followed by several other attempts [19,21] that either failed in parts of the phase space or were not general enough to be applied to any liquid. Also attempts to obtain the pair interaction by fitting a parametrized potential via computer simulation to experimental structure data should be mentioned here [17]. In contrast to all these attempts the method proposed by Levesque and co-workers overcomes all these drawbacks (at least in the one-component case): it can be applied to any simple liquid and gives reliable results even near the triple point, i.e., in a region of the phase diagram, where the structure is not too sensitive to the interatomic potential and the inversion problem is hence very difficult to solve accurately. Although the generalization of the formalism to the binary case is straightforward, its realization is by no means trivial and even fails in some cases: in a recent study it was shown [25] that for the case of small minority concentrations the statistical errors in the computer simulation step accumulate and do not lead to satisfactory results. Furthermore, the required ''extension'' of the simulation data over a larger r range also bears some arbitrariness in itself. To overcome the problem of small concentrations we would require larger ensembles, which, despite the computational power of present-day workstations, soon brings us to natural limits. On the other hand, smoothing of the simulation data leads to a biasing [26] of the results and therefore not to very satisfactory results either.

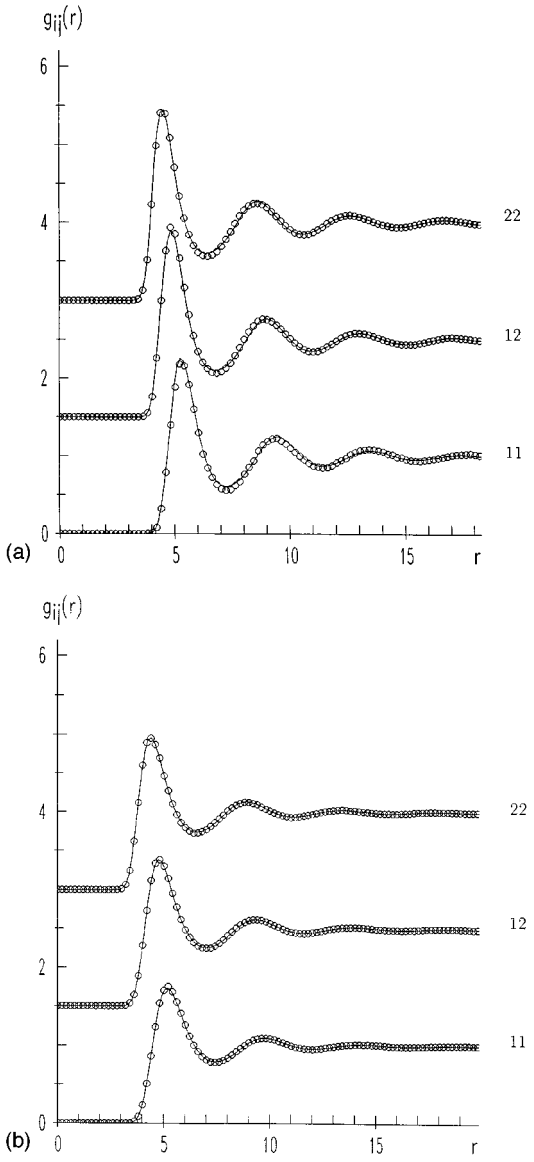

FIG. 6. Partial PDFs $g_{ij}(r)$ (as labeled) as functions of r (in angstroms) for two K_cCs_{1-c} alloys considered in our study: (a) $c=0.8$ and $T=373$ K and (b) $c=0.4$ and $T=773$ K; for further parameters cf. Table III. Symbols denote the following: ○, MD data; lines, present study.

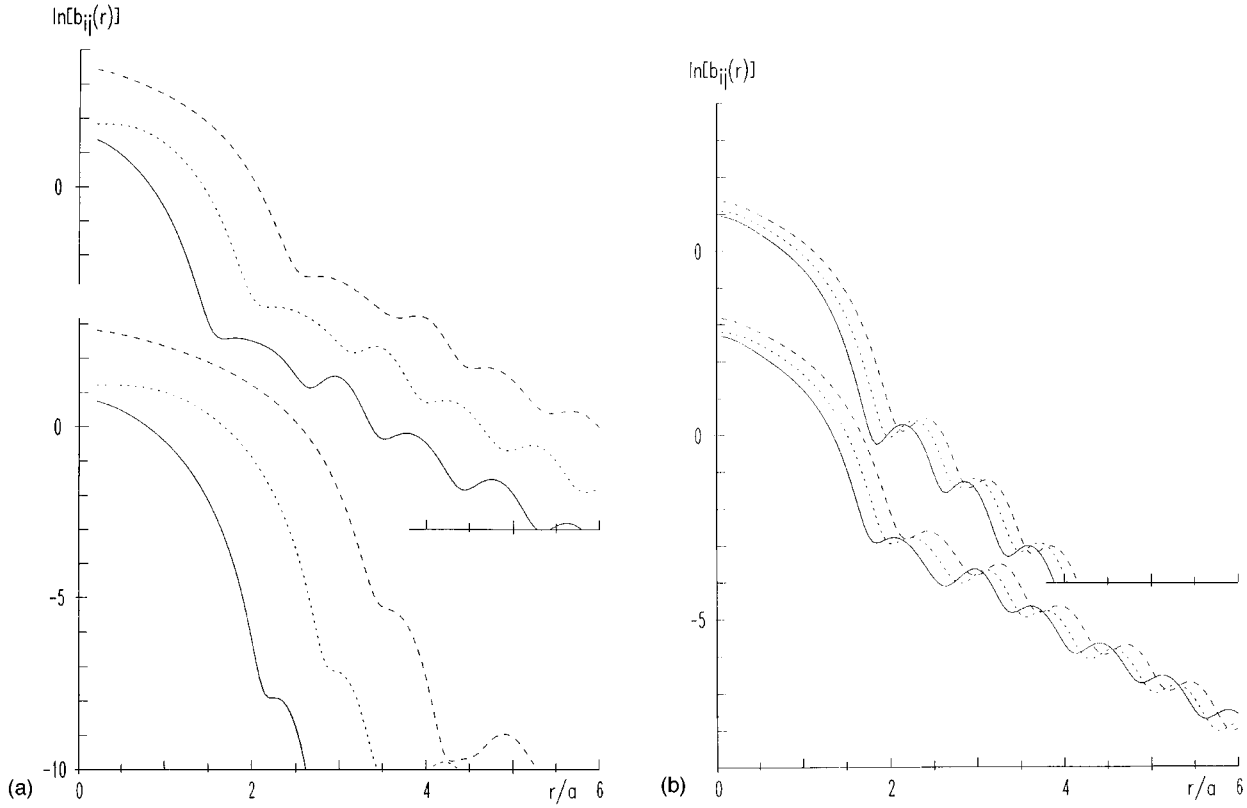

FIG. 7. $\ln[b_{ij}(r)]$ vs r/a (a being the Wigner-Seitz radius) for four different systems (11, full line; 12, dotted line; and 22, broken line). η is the packing fraction of the HS reference system taken from the respective tables. (a) Binary ionic mixtures as characterized by parameters of Table I: top, $c_2=0.5$ and $\eta=0.451$; bottom, $c_2=0.05$ and $\eta=0.292$. (b) Binary alloys (for system parameters cf. Table III): top, $T=373$ K, $c_K=0.2$, and $\eta=0.45$; bottom, $T=973$ K, $c_K=0.7$, and $\eta=0.28$.

Since we have shown in Sec. III A that our approach proposed here is able to yield results as accurate as computer simulations, we have replaced the simulation step in the inversion scheme by our method and checked the reliability of the results. The predictor-corrector inversion scheme works as follows. We are given a set of ''experimental'' structure data $\{g_{11}(r),g_{22}(r),g_{12}(r)\}=\mathbf{g}^0=\mathbf{g}^{\text{expt}}$ from which we can also calculate, via the Ornstein-Zernike equations, the direct correlation functions $\mathbf{c}^0=\mathbf{c}^{\text{expt}}$; we assume that these functions are ''produced'' by the set of interatomic potentials $\mathbf{\Phi}^0$, which are still unknown and which we want to determine in this procedure. In practical applications (as, e.g., in [24]) the $\mathbf{g}^0$ are known from experimental scattering data; here, where we would like to test the reliability of our method, these data have been produced in a computer experiment using the pair interactions $\mathbf{\Phi}^0$. From $\mathbf{g}^0$ we determine, e.g., via some liquid state theory (PY or MHNC approximation), a set of interactions $\mathbf{\Phi}^1$, i.e., a predictor (or first guess) for $\mathbf{\Phi}^0$. The subsequent (corrector) step is a computer simulation (replaced in this work by our method) performed for a system characterized by $\mathbf{\Phi}^1$, yielding the PDFs $\mathbf{g}^1$. Using the universality hypothesis of the bridge functions [12] one can now construct a new predictor $\mathbf{\Phi}^2$ for $\mathbf{\Phi}^0$ and thus ends up in an iterative formalism that enables us to calculate the potentials $\mathbf{\Phi}^k$ from the $\mathbf{\Phi}^{k-1}$, i.e., the potentials of the preceding step:

$$\Phi_{ij}^k(r)=\Phi_{ij}^{k-1}(r)+\ln[g_{ij}^{k-1}(r)/g_{ij}^{\text{expt}}(r)]+c_{ij}^{k-1}(r)-c_{ij}^{\text{expt}}(r)-g_{ij}^{k-1}(r)+g_{ij}^{\text{expt}}(r). \tag{23}$$

The sequence of the $\mathbf{\Phi}^k$ should tend towards $\mathbf{\Phi}^0$. As mentioned above, the crucial point in the binary case is the corrector step, i.e., the simulation step. In this work we have replaced this simulation by our integral-equation method, where small concentrations do not affect the reliability of the results.

We have investigated several systems and present results for three of them (A, B, and C). They are again Ar-Kr mixtures characterized by LJ potentials [cf. (21)]; their system parameters are compiled in Table IV. In particular, systems

TABLE IV. Potential parameters ε_{ij}^* and σ_{ij} ($ij=1,2$) of the three LJ systems investigated (A–C) in the inversion section. c_1 is the concentration of species 1. The mass of atom 1 (2) is that of Ar (Xe), i.e., 6.682×10^{-26} kg (2.180×10^{-25} kg) and the mass density is for all systems 1874 kg m^{-3}. N is the number of particles in the MD simulation.

System	ε_{11}^*	ε_{12}^*	ε_{22}^*	σ_{11}/σ_{22}	σ_{12}/σ_{22}	c_1	N
A	0.4278	0.6278	0.8278	0.873	0.936	5/8	4000
B	0.4278	0.6278	0.8278	0.873	0.936	1/10	6912
C	0.4278	0.6278	0.8278	0.873	0.936	1/20	16384

B and C have been chosen with small minority concentrations ($c_1=0.1$ and $c_1=0.05$) in an effort to demonstrate that the present version of the inversion scheme yields reliable results even for such cases. The experimental data have been produced in standard MD simulation runs (see above) over 20 000 time steps with the number of particles indicated in Table IV. From this table one can also see that the number of particles has been increased with decreasing minority concentration in order to guarantee a high accuracy of the experimental data. The $\mathbf{g}^0$ have been extended beyond the cutoff radius $r_{\rm cut}=4\sigma_{22}$ of the simulations by two different closure relations, i.e., $c_{ij}^0(r)=0$ and $c_{ij}^0(r)=-\beta\Phi_{ij}^0(r)$.

Note that for smooth data (i.e., with little statistical noise) for the PDFs, the inversion problem is solved in *one* iteration within the approximation of universality of the bridge functional: inserting the experimental $\mathbf{g}^0$ into the bridge functional, we get the bridge functions as functions of the reference parameters, which are then optimized by the Lado equations. With thus specified $\underline{b}_{ij}(r)$ we just employ the MHNC closure and the Ornstein-Zernike relations and obtain the potentials $\Phi_{ij}(r)$ from the experimental $g_{ij}^0(r)$. Applying this procedure to the $g_{ij}(r)$'s specified above reproduces quite accurately the correct potentials in Fig. 8(a) [denoted as $\underline{\Phi}_{ij}^1(r)$]. The accuracy obtained by this procedure depends of course on the accuracy (i.e., in our case on the statistical error) of the PDFs; in this figure we have therefore displayed the results system B with a minority concentration of 0.1. Despite the good results of this first guess we have demonstrated the robustness of the method by a *deliberate* distortion (''by hand'') of the initial guess of the predictor-corrector scheme.

The first guess for the potential $\mathbf{\Phi}^1$ in the predictor-corrector scheme has been obtained by deliberately modifiying the original interactions $\mathbf{\Phi}^0$ by hand. For simplicity we have assumed the same $\mathbf{\Phi}^1$ for all systems; $\mathbf{\Phi}^0$ and $\mathbf{\Phi}^1$ are depicted in Fig. 8(a). By applying the inversion procedure outlined above we create a sequence of $\mathbf{\Phi}^i$. The results are depicted in Figs. 8(b)–8(d) for systems A–C. For the first system we got a satisfactory solution after four steps. The small oscillations observed in the potentials in the region $1.5\sigma_{22}$–$1.8\sigma_{22}$ are due to the size effects of the MD results; they are much weaker in system B, where a larger ensemble has been considered. For system B a satisfactory convergence of the algorithm is observed after three steps. For system C (characterized by the smallest minority concentration $c_1=0.05$, corresponding to $\sim$800 particles of type 1) we obtained again satisfactory results after three iterations. Only near $\sim 1.8\sigma_{22}$ oscillations are visible that have to be attributed to the statistical errors in the simulation data for $g_{11}(r)$. In general, the results turn out to be rather insensitive to the closure used for the extension of the experimental data. However, a grid of at least 1024 points and of a mesh size of 0.01 (in Wigner-Seitz radii a) is recommendable to obtain the displayed accuracy.

The advantages of using the integral-equation approach instead of the simulation in the iterative procedure are quickly summarized: the present version is much faster since simulations for ensembles of 7000 particles (or even more) over several thousands of time steps are still very time consuming. In addition, every simulation (representing the corrector step) introduces some additional statistical error, which in the end do not cancel out but rather accumulate; this results in a higher number of iteration steps (i.e., 12 instead of 3–4) and statistical errors (i.e., rapid oscillations) even for intermediate concentrations (cf. Figs. 1–3 in [25]). The crucial basis for a successful and rapid convergence of the algorithm remains (in both cases) accurate and reliable input data of the structure.

IV. CONCLUSION

In this paper we have investigated an integral-equation approach to determine the structure and thermodynamics of a binary mixture of simple liquids. In this method the Ornstein-Zernike equations are solved along with a MHNC-RHNC-type closure relation where the bridge functions are calculated from an (approximate) bridge functional, which, in turn, is calculated from a model free-energy functional for the reference system. The basic assumption of our method is the universality hypothesis at the level of the bridge *functional* (which is easily obtainable via functional derivative from the free-energy functional). In contrast to previous MHNC and RHNC calculations (where universality was assumed at the level of the bridge *functions*) the bridge functions used here contain (via the functional) the structure of both the reference system and the system under consideration. As a reference system we have chosen a mixture of additive HS for which, as shown recently, an expression for the excess free-energy functional based on fundamental geometric properties of the individual spheres can be constructed. This functional may be applied, in its most general case, to inhomogeneous liquids and reproduces in the homogeneous case the expressions based on the analytic PY solution and the scaled particle theory. As a result of the accuracy of the bridge functional and the universality hypothesis, a Lado-type criterion guarantees a high degree of thermodynamic self-consistency.

The reliability and numerical accuracy of this method was tested for several model liquids (HS, binary Coulombic systems, LJ mixtures, and binary liquid alkali alloys) over a vast range of parameters; these parameters were also chosen so as to create a strongly nonadditive system, with respect to both the distance and energy parameters. Numerical results were compared with simulation data (Monte Carlo and MD simulations) taken either from literature or produced for this work. In general, agreement is very satisfactory, even for strongly nonadditive systems. Problems were encountered for those parameter combinations where simulations and other liquid state methods predict a near phase separation. The answer to the question how accurately our method is able to reproduce phase stability and phase diagrams must be postponed to a later study. Our results demonstrate that, within numerical accuracy, the present method based on universality of the bridge functional is as accurate and reliable as present day simulations.

In order to substantiate this ''claim'' in a practical application we have replaced computer simulation by this approach in an algorithm to solve the classical inversion problem in liquid state theory. The method chosen is an iterative algorithm proposed some years ago by Levesque *et al.* and represents at present the most reliable tool to solve this non-

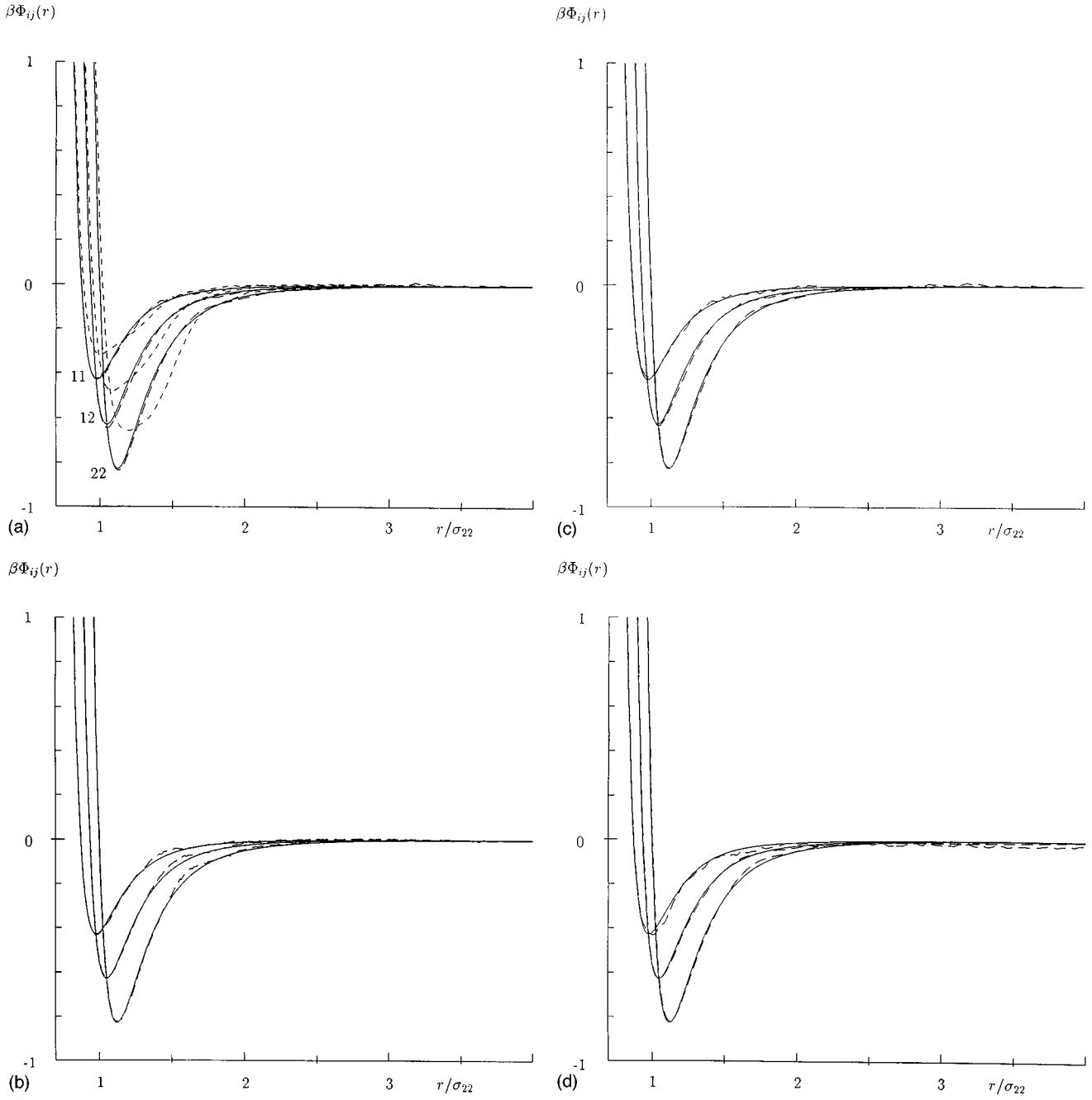

FIG. 8. (a) Interatomic potentials (as labeled) $\mathbf{\Phi}^0$ (initial potential, full line), $\mathbf{\Phi}^1$ (first guess by deliberate distortion, broken line), and $\overline{\mathbf{\Phi}}^1$ (first guess as described in the text, long-dashed line) used in this contribution for the inversion scheme as functions of r in units σ_{22}. (b) Comparison of the initial potentials $\mathbf{\Phi}^0$ (full line) with the (converged) $\mathbf{\Phi}^4$ (broken line) for system A [for labels cf. (a)]. (c) Comparison of the initial potentials $\mathbf{\Phi}^0$ (full line) with the (converged) $\mathbf{\Phi}^3$ (broken line) for system B [for labels cf. (a)]. (d) Comparison of the initial potentials $\mathbf{\Phi}^0$ (full line) with the (converged) $\mathbf{\Phi}^3$ (broken line) for system C [for labels see (a)].

trivial problem. One iteration consists of a predictor and a corrector step, where, as proposed in the original work, the corrector step is realized by a computer simulation. In this work we have replaced this simulation by our approximate method and find that it indeed can be used in this framework and that the iterative algorithm converges in a very satisfactory way. In addition, and in contrast to simulations, the inversion scheme using our method in the corrector step gives reliable results for those system parameters where simulations fail, i.e., for small minority components. From the numerical point of view the algorithm turned out to be rather robust and can, in principle, although with a considerable formal effort (which might be achieved by use of formal languages, such as MATHEMATICA), be generalized to more-component systems.

On the basis of all those comparisons we may conclude that by capturing the correct geometrical features, the fundamental-measure bridge functional leads to an accurate description of all types of homogeneous simple liquid mixtures of which the pair correlation functions can be grossly

interpreted in terms of effective hard-core repulsions. Molten salts and electrolytes, when they feature pair correlation functions with very strong nonadditivity of the effective spheres, cannot be expected to be similarly well represented by the HS bridge functional and will be considered in a separate work.

ACKNOWLEDGMENTS

Y.R. thanks the members of the Physics Department of Bristol University, in particular Professor Bob Evans, for their warm hospitality and the Benjamin Meaker Foundation for generous support. Interesting discussions with Bob Evans are acknowledged with gratitude. This work was supported in part by the Österreichische Forschungsfonds under Projects Nos. P8912-PHY and P11194-PHY. The authors are indebted to H.E. DeWitt, W.L. Slattery, G. Chabrier, J. Jung, M.S. Jhon, and F.H. Ree for sending us detailed computer simulation data prior to publication.

APPENDIX A: THE FREE-ENERGY FUNCTIONAL

The geometrically based fundamental measure functional takes the form [7,8,15]

$$\frac{1}{k_BT}F_{\rm ex}^{\rm HS}[\boldsymbol{\rho}]=\int d\mathbf{r}\,\Phi\{\mathbf{n}(\mathbf{r})\}, \tag{A1}$$

where Φ is a *function* of a set of weighted densities $\{\mathbf{n}(\mathbf{r})\}=(n_0,n_1,\ldots,n_\alpha,\ldots)$ related to the set of density profiles $\{\boldsymbol{\rho}\}$ via

$$\mathbf{n}_\alpha(r)=\sum_i\int d\mathbf{r}'\rho_i(r')\boldsymbol{\omega}_i^{(\alpha)}(\mathbf{r}-\mathbf{r}') \tag{A2}$$

and the weight functions $\{\boldsymbol{\omega}_i^{(\alpha)}(\mathbf{r}')\}$ are characteristic functions for the geometry of the particles. For a three-dimensional sphere of radius R_i the set of weight functions is

$$\begin{aligned}
\omega_i^{(0)}(\mathbf{r})&=\frac{1}{4\pi R_i^2}\omega_i^{(2)}(\mathbf{r}),\\
\omega_i^{(1)}(\mathbf{r})&=\frac{1}{4\pi R_i}\omega_i^{(2)}(\mathbf{r})=|\boldsymbol{\omega}_i^{(1)}(\mathbf{r})|,\\
\omega_i^{(2)}(\mathbf{r})&=\delta(R_i-|\mathbf{r}|)=|\boldsymbol{\omega}_i^{(2)}(\mathbf{r})|,\\
\omega_i^{(3)}(\mathbf{r})&=\Theta(R_i-|\mathbf{r}|),\\
\boldsymbol{\omega}_i^{(1)}(\mathbf{r})&=\frac{1}{4\pi R_i}\boldsymbol{\omega}_i^{(2)}(\mathbf{r}),\\
\boldsymbol{\omega}_i^{(2)}(\mathbf{r})&=\frac{\mathbf{r}}{r}\delta(R_i-|\mathbf{r}|),
\end{aligned} \tag{A3}$$

where the first four equations are the scalar weight functions, and the last two equations are the vector wave functions. In principle $\omega_i^{(3)}(\mathbf{r})$, $\omega_i^{(2)}(\mathbf{r})$, and $\boldsymbol{\omega}_i^{(2)}(\mathbf{r})$ are sufficient to calculate the full set $\{\boldsymbol{\omega}_i^{(\alpha)}\}$.

The convolution integrals are most readily performed in q space, where they reduce to products of the Fourier transforms of the two functions involved. The Fourier transforms of the weight functions (denoted by a tilde) are given by

$$\begin{aligned}
\tilde{\omega}_i^{(0)}(q)&=\frac{\sin(qR_i)}{qR_i}R_i^{(0)},\\
\tilde{\omega}_i^{(1)}(q)&=\frac{\sin(qR_i)}{qR_i}R_i^{(1)},\\
\tilde{\omega}_i^{(2)}(q)&=\frac{\sin(qR_i)}{qR_i}R_i^{(2)},\\
\tilde{\omega}_i^{(3)}(q)&=3\frac{\sin(qR_i)-(qR_i)\cos(qR_i)}{(qR_i)^3}R_i^{(3)}.\\
\tilde{\boldsymbol{\omega}}_i^{(1)}(q)&=\frac{1}{4\pi R_i}\tilde{\boldsymbol{\omega}}_i^{(2)}(q),\\
\tilde{\boldsymbol{\omega}}_i^{(2)}(q)&=-1\sqrt{-1}\,\mathbf{q}\tilde{\omega}_i^{(3)}(q),
\end{aligned} \tag{A4}$$

The $R_i^{(\gamma)}$, $\gamma=0,\ldots,3$, describe characteristic geometric features of the *individual* spheres

$$\begin{aligned}
R_i^{(0)}&=1,\quad R_i^{(2)}=4\pi R_i^2,\\
R_i^{(1)}&=R_i,\quad R_i^{(3)}=\frac{4\pi}{3}R_i^3.
\end{aligned} \tag{A5}$$

Furthermore, one finds for the limits $q\to 0$

$$\lim_{q\to 0}\tilde{\omega}_i^{(\gamma)}(q)=R_i^{(\gamma)},\quad \lim_{q\to 0}\tilde{\boldsymbol{\omega}}_i^{(\gamma)}(q)=\mathbf{0}. \tag{A6}$$

It is then obvious that in the uniform limit the scalar densities $n_\alpha(\mathbf{r})$ become

$$n_\gamma(\mathbf{r})\to\xi_\gamma=\sum_i\rho_iR_i^\gamma,\quad \gamma=0,\ldots,3, \tag{A7}$$

while the vector densities $\mathbf{n}_\gamma(\mathbf{r})$ vanish in this limit. In particular, $\xi_3=\eta$, the packing fraction.

One finds finally that $\Phi\{\mathbf{n}(\mathbf{r})\}$ is given by [7,8,15]

$$\begin{aligned}
\Phi\{\mathbf{n}(\mathbf{r})\}=&-n_0\ln(1-n_3)+\frac{n_1n_2}{(1-n_3)}+\frac{1}{24\pi}\frac{n_2^3}{(1-n_3)^2}\\
&-\frac{\mathbf{n}_1\cdot\mathbf{n}_2}{1-n_3}-\frac{1}{8\pi}\frac{n_2(\mathbf{n}_2\cdot\mathbf{n}_2)}{(1-n_3)^2}.
\end{aligned} \tag{A8}$$

Again the first line contains the scalar contributions, while the second line represents the vector contributions. It is possible to construct a ''simplified'' free-energy model with a different set of entirely *scalar* weight functions [57], requiring, however, the inclusion of derivatives of generalized functions. The equivalence of this simplified model and the original (present) one has been shown explicitly in [58], where also a detailed comparison between both versions of the model is done.

As already outlined in Sec. II A [Eqs. (4) and (5)], density-functional theory provides the possibility to calculate the direct correlation functions $c^{(n),\mathrm{FD}}_{1,\ldots,n}[\boldsymbol{\rho}](\mathbf{r}_1,\ldots,\mathbf{r}_n)$ via the functional derivative of the excess free-energy functional $F_{\mathrm{ex}}[\boldsymbol{\rho}]$ with respect to the one-particle densities $\rho_i(\mathbf{r}_k)$. One then obtains the general expressions

$$
\begin{aligned}
&c^{(n)}(\mathbf{r}_1,\ldots,\mathbf{r}_n)\\
&\quad=-\int d\mathbf{r}\sum_{\alpha_1,\ldots,\alpha_n}\left[\frac{\partial\Phi}{\partial n_{\alpha_1}\cdots\partial n_{\alpha_n}}\right|_{\{n_\alpha\}=\{n_\alpha(\mathbf{r})\}}](\mathbf{r})\\
&\qquad\times\omega_1^{(\alpha_1)}(\mathbf{r}_1-\mathbf{r})\cdots\omega_n^{(\alpha_n)}(\mathbf{r}_n-\mathbf{r})\\
&\qquad-\int d\mathbf{r}\sum_{\beta_1,\ldots,\beta_n}\left[\frac{\partial\Phi}{\partial \mathbf{n}_{\beta_1}\cdots\partial \mathbf{n}_{\beta_n}}\right|_{\{\mathbf{n}_\beta\}=\{\mathbf{n}_\beta(\mathbf{r})\}}](\mathbf{r})\\
&\qquad\times\boldsymbol{\omega}_1^{(\beta_1)}(\mathbf{r}_1-\mathbf{r})\cdots\boldsymbol{\omega}_n^{(\beta_n)}(\mathbf{r}_n-\mathbf{r}),
\end{aligned}
\tag{A9}
$$

$$
\begin{aligned}
&\tilde{c}^{(n)}(\mathbf{q}_1,\ldots,\mathbf{q}_n)\\
&\quad=-\sum_{\alpha_1,\ldots,\alpha_n}\left[\frac{\partial\Phi}{\partial n_{\alpha_1}\cdots\partial n_{\alpha_n}}\right]_{\{n_\alpha\}=\{\xi_\alpha\}}\\
&\qquad\times\tilde{\omega}_1^{(\alpha_1)}(\mathbf{q}_1)\cdots\tilde{\omega}_n^{(\alpha_n)}(\mathbf{q}_n)\,\delta\Big(\sum_i\mathbf{q}_i=\mathbf{0}\Big)\\
&\qquad-\sum_{\alpha_1,\ldots,\alpha_n}\left[\frac{\partial\Phi}{\partial \mathbf{n}_{\alpha_1}\cdots\partial \mathbf{n}_{\alpha_n}}\right]_{\{n_\alpha\}=\{\xi_\alpha\}}\\
&\qquad\times\tilde{\boldsymbol{\omega}}_1^{(\alpha_1)}(\mathbf{q}_1)\cdots\tilde{\boldsymbol{\omega}}_n^{(\alpha_n)}(\mathbf{q}_n)\,\delta\Big(\sum_i\mathbf{q}_i=\mathbf{0}\Big),
\end{aligned}
\tag{A10}
$$

again separated into scalar and vectorial contributions.

In particular one obtains for $n=1$ and $n=2$ the expressions in the homogeneous case [59,60]

$$
-c_i^{(1)}(r)=-(k_BT)^{-1}\mu_{i,\mathrm{ex}}=-\sum_\alpha\mu^\alpha R_i^\alpha,
\tag{A11}
$$

$$
\begin{aligned}
-c_{ij}^{(2)}(r)=&\chi^{(3)}\Delta V_{ij}(r)+\chi^{(2)}\Delta S_{ij}(r)+\chi^{(1)}\Delta R_{ij}(r)\\
&+\chi^{(0)}\Theta[r-(R_i+R_j)].
\end{aligned}
\tag{A12}
$$

The coefficients μ_i^α and $\chi^{(\alpha)}$ are functions of the ξ_k and are explicitly given by

$$
\begin{aligned}
&\mu^{(0)}=-\ln(1-\xi_3),\quad \mu^{(1)}=\frac{\xi_2}{(1-\xi_3)},\\
&\mu^{(2)}=\frac{\xi_1}{(1-\xi_3)}+\frac{1}{8\pi}\frac{\xi_2^2}{(1-\xi_3)^2},\\
&\mu^{(3)}=\frac{\xi_0}{(1-\xi_3)}+\frac{\xi_1\xi_2}{(1-\xi_3)^2}+\frac{1}{12\pi}\frac{\xi_2^3}{(1-\xi_3)^3},\\
&\chi^{(0)}=\frac{1}{(1-\xi_3)},\quad \chi^{(1)}=\frac{\xi_2}{(1-\xi_3)^2},\\
&\chi^{(2)}=\frac{\xi_1}{(1-\xi_3)^2}+\frac{1}{4\pi}\frac{\xi_2^2}{(1-\xi_3)^3},\\
&\chi^{(3)}=\frac{\xi_0}{(1-\xi_3)^2}+\frac{2\xi_1\xi_2}{(1-\xi_3)^3}+\frac{1}{4\pi}\frac{\xi_2^3}{(1-\xi_3)^4}.
\end{aligned}
\tag{A13, A14}
$$

The factors of the $\chi^{(\gamma)}$ in (A12) now represent characteristic quantities of the *pair* exclusion volume of two spheres with radii R_i and R_j at a distance r from each other [e.g., $\Delta V_{ij}(r)$ is the overlap volume and $\Delta S_{ij}(r)$ is the overlap surface]. $c_{ij}^{(2)}(r)$ in (35) is identical to the analytic expression obtained by Lebowitz and Rowlinson [39] within the PY approximation. The uniform fluid $c^{(3)}$ has been favorably compared with computer simulations [60,61].

APPENDIX B: THE LADO CRITERION

Introducing a reference system, we can rewrite Eq. (6) as

$$
F_{\mathrm{ex}}[\boldsymbol{\rho}]=F_{\mathrm{ex}}^{(2)}[\boldsymbol{\rho}_0;\boldsymbol{\rho}]+\big[F_{\mathrm{ex}}^{(2)}[\boldsymbol{\rho}_0;\boldsymbol{\rho}]-F_{\mathrm{ex}}^{(2),\mathrm{ref}}[\boldsymbol{\rho}_0;\boldsymbol{\rho}]\big],
\tag{B1}
$$

where the term in bold square brackets represents the functional $F_{\mathrm{ex}}^{(\mathrm{B}),\mathrm{ref}}[\boldsymbol{\rho}]$, which generates the bridge functional of the reference system $B_i^{\mathrm{ref}}[\boldsymbol{\rho}_0;\mathbf{g}](\mathbf{r})$.

In the above equations the second-order functionals for the system and the reference system can be calculated *in the bulk* (due to the absence of the bridge functions) from the HNC expression for the free-energy functional, i.e.,

$$
F_{\mathrm{ex}}[\boldsymbol{\rho}_0]=F^{\mathrm{ref}}[\boldsymbol{\rho}_0]+F_{\mathrm{HNC}}[\boldsymbol{\rho}_0]-F_{\mathrm{HNC}}^{\mathrm{ref}}[\boldsymbol{\rho}_0].
\tag{B2}
$$

The explicit expressions for these functionals are given in [62,63].

As demonstrated in [63], the PDFs $g_{ij}(r)$, obtained from a HNC solution of the OZ equations for a given set of potentials $\Phi_{ij}(r)$, guarantee that the variation of the HNC functional $F_{\mathrm{HNC}}[\boldsymbol{\rho}_0]$ is given by

$$
\delta F_{\mathrm{HNC}}[\boldsymbol{\rho}_0]=\frac{\rho}{2k_BT}\sum_{i,j}c_ic_j\int d\mathbf{r}\,g_{ij}(r)\,\delta\Phi_{ij}(r).
\tag{B3}
$$

Since the bulk limit of the optimized free energy is the solution of HNC equations with the effective interactions $\{\Phi_{ij}^{\mathrm{eff}}(r)+\overline{b_{ij}^{\mathrm{ref}}}(r)\}$ (for $F_{\mathrm{HNC}}^{\mathrm{ref}}[\boldsymbol{\rho}_0]$) and $\{\Phi_{ij}(r)+\overline{b_{ij}^{\mathrm{ref}}}(r)\}$ (for $F_{\mathrm{HNC}}[\boldsymbol{\rho}_0]$), respectively, we obtain

$$
\delta F_{\mathrm{HNC}}[\boldsymbol{\rho}_0]=\frac{\rho}{2k_BT}\sum_{i,j}c_ic_j\int d\mathbf{r}\,g_{ij}(r)\,\delta\overline{b_{ij}^{\mathrm{ref}}}(\mathbf{g};r),
\tag{B4}
$$

$$
\delta F_{\mathrm{HNC}}^{\mathrm{ref}}[\boldsymbol{\rho}_0]=\frac{\rho}{2k_BT}\sum_{i,j}c_ic_j\int d\mathbf{r}\,g_{ij}^{\mathrm{ref}}(r)[\,\delta\Phi_{ij}^{\mathrm{ref}}(r)
$$

$$+\delta\overline{b}_{ij}^{\mathrm{ref}}(\mathbf{g}^{\mathrm{ref}};r)]. \tag{B5}$$

Relation (B3) holds, furthermore, for the variation of the exact free-energy functional with respect to the variation in the $\Phi_{ij}(r)$, i.e.,

$$\delta F^{\mathrm{ref}}[\boldsymbol{\rho}_0]=\frac{\rho}{2k_BT}\sum_{i,j}\, c_ic_j\int d\mathbf{r}\, g_{ij}^{\mathrm{ref}}(r)\,\delta\Phi_{ij}^{\mathrm{ref}}(r). \tag{B6}$$

Adding these three terms according to (B1) we obtain

$$\delta F[\boldsymbol{\rho}_0]=\frac{\rho}{2k_BT}\sum_{i,j}\, c_ic_j\int d\mathbf{r}[g_{ij}(r)\,\delta\overline{b}_{ij}^{\mathrm{ref}}(\mathbf{g};r) - g_{ij}^{\mathrm{ref}}(r)\,\delta\overline{b}_{ij}^{\mathrm{ref}}(\mathbf{g}^{\mathrm{ref}};r). \tag{B7}$$

Concluding on the basic assumption of our method that the bridge functional is relatively insensitive to the actual shape of the input PDFs [i.e., $\delta\overline{b}_{ij}^{\mathrm{ref}}(\mathbf{g};r)\sim\delta\overline{b}_{ij}^{\mathrm{ref}}(\mathbf{g}^{\mathrm{ref}};r)$], we finally obtain

$$\delta F[\boldsymbol{\rho}_0]=\frac{\rho}{2k_BT}\sum_{i,j}\, c_ic_j\int d\mathbf{r}[g_{ij}(r)-g_{ij}^{\mathrm{ref}}(r)]\,\delta\overline{b}_{ij}^{\mathrm{ref}}(\mathbf{g};r). \tag{B8}$$

The optimal choice of the reference system makes $\delta F[\boldsymbol{\rho}_0]$ stationary with respect to the variation of the reference system parameters and leads to Eq. (16).

[1] J.-P. Hansen and I.R. McDonald, *Theory of Simple Liquids*, 2nd ed. (Academic, New York, 1986).

[2] J. Talbot, J.L. Lebowitz, E.M. Waisman, D. Levesque, and J.-J. Weis, J. Chem. Phys. **85**, 2187 (1986); G. Pastore and G. Kahl, J. Phys. F **17**, L267 (1987).

[3] E. Enciso, F. Lado, M. Lombardero, J.L.F. Abascal, and S. Lago, J. Chem. Phys. **87**, 2249 (1987).

[4] G. Kahl, Phys. Rev. A **43**, 822 (1991).

[5] J.-A. Anta and G. Kahl, Mol. Phys. **84**, 1273 (1995).

[6] E. Lomba, M. Alvarez, L.L. Lee, and N.G. Almarza, J. Chem. Phys. **104**, 4180 (1996).

[7] Y. Rosenfeld, J. Chem. Phys. **98**, 8126 (1993).

[8] Y. Rosenfeld, Phys. Rev. Lett. **72**, 3831 (1994); J. Phys. Chem. **99**, 2857 (1995).

[9] Y. Rosenfeld, in *Physics of Strongly Coupled Plasma Physics*, edited by W. Kraeft and M. Schlanges (World Scientific, Singapore, 1996), pp. 27–36.

[10] Y. Rosenfeld, Phys. Rev. E **54**, 2827 (1996).

[11] F. Lado, S.M. Foiles, and N.W. Ashcroft, Phys. Rev. A **28**, 2374 (1983).

[12] Y. Rosenfeld and N.W. Ashcroft, Phys. Rev. A **20**, 1208 (1979).

[13] M.S. Wertheim, Phys. Rev. Lett. **10**, 321 (1963); J. Math. Phys. **5**, 643 (1964); E. Thiele, J. Chem. Phys. **39**, 474 (1963).

[14] L. Verlet and J.-J. Weis, Phys. Rev. A **5**, 939 (1972); D. Henderson and E.W. Grundke, J. Chem. Phys. **63**, 601 (1975).

[15] Y. Rosenfeld, Phys. Rev. Lett. **63**, 980 (1989).

[16] J.K. Percus, Phys. Rev. Lett. **8**, 462 (1962); J.K Percus, in *The Equilibrium Theory of Classical Fluids*, edited by H.L. Frisch and J.L. Lebowitz (Benjamin, New York, 1964), p. II-171.

[17] M. Dzugutov, K.-E. Larsson, and I. Ebbsjö, Phys. Rev. A **38**, 3609 (1988).

[18] M.D. Johnson, P. Hutchinson, and N.H. March, Proc. R. Soc. London, Ser. A **282**, 283 (1964).

[19] W. Schommers, Phys. Rev. A **28**, 3599 (1983).

[20] S. Kambayashi and J. Chihara, Phys. Rev. E **50**, 1317 (1994).

[21] M.W.C. Dharma-wardana and G.C. Aers, Phys. Rev. B **28**, 1701 (1983).

[22] D. Levesque, J.-J. Weis, and L. Reatto, Phys. Rev. Lett. **54**, 451 (1985); M.W.C. Dharma-wardana and G.C. Aers, *ibid.* **56**, 1211 (1986); D. Levesque, J.-J. Weis, and L. Reatto, *ibid.* **56**, 1212 (1986).

[23] L. Reatto, D. Levesque, and J.-J. Weis, Phys. Rev. A **33**, 3451 (1986).

[24] M.C. Bellisent-Funel, P. Chieux, D. Levesque, and J.-J. Weis, Phys. Rev. A **39**, 6310 (1989).

[25] G. Kahl and M. Kristufek, Phys. Rev. E **49**, R3568 (1994).

[26] G. Kahl (unpublished).

[27] R. Evans, Adv. Phys. **28**, 143 (1979); in *Fundamentals of Inhomogeneous Fluids*, edited by D. Henderson (Dekker, New York, 1992).

[28] H.C. Andersen, D. Chandler, and J.D. Weeks, Adv. Chem. Phys. **34**, 105 (1976).

[29] J.L. Lebowitz, Phys. Rev. A **133**, 895 (1964).

[30] J.K. Percus, J. Stat. Phys. **52**, 1157 (1988); L. Blum and Y. Rosenfeld, *ibid.* **63**, 1177 (1991).

[31] C. Tutschka (unpublished); J.K. Percus (private communication).

[32] F. Lado, Phys. Rev. A **8**, 2548 (1973).

[33] F. Lado, Phys. Lett. A **89**, 196 (1982).

[34] G. Pastore and G. Senatore (unpublished).

[35] M. Gillan, Mol. Phys. **38**, 1781 (1979).

[36] J. Jung, M.S. Jhon, and F.H. Ree, J. Chem. Phys. **100**, 9064 (1994).

[37] J. Jung, M.S. Jhon, and F.H. Ree, J. Chem. Phys. **102**, 1349 (1995).

[38] H.E. DeWitt, W.L. Slattery, and G. Chabrier, Physica B (to be published).

[39] J.L. Lebowitz and J.S. Rowlinson, J. Chem. Phys. **41**, 133 (1964).

[40] T. Biben and J.-P. Hansen, Phys. Rev. Lett. **66**, 2215 (1991); T. Biben and J.-P. Hansen, J. Phys. Condens. Matter **3**, F65 (1991); T. Biben, Ph.D thesis, Université Claude Bernard, Lyon, 1992 (unpublished).

[41] D. Gazillo, J. Chem. Phys. **95**, 4565 (1991); D. Gazillo, Mol. Phys. **84**, 303 (1995).

[42] M. Rovere and G. Pastore, J. Phys. Condens. Matter **6**, A163 (1994).

[43] P. Ballone, G. Pastore, G. Galli, and D. Gazillo, Mol. Phys. **59**, 275 (1986).

[44] I.R. McDonald, Mol. Phys. **23**, 41 (1972).

[45] B.P. Alblas, W. van der Lugt, O. Mensies, and C. van Dijk, Physica B **106**, 22 (1981).
[46] G. Kahl and J. Hafner, J. Phys. F **15**, 1627 (1985).
[47] G. Kahl and J. Hafner, Phys. Chem. Liq. **17**, 139 (1987).
[48] H. Mori, K. Hoshino, and M. Watabe, J. Non-Cryst. Solids **156-158**, 85 (1993).
[49] N.W. Ashcroft, Phys. Lett. **23**, 48 (1966).
[50] S. Ichimaru and K. Utsumi, Phys. Rev. B **24**, 7381 (1981).
[51] J. Hafner, *From Hamiltonians to Phase Diagrams* (Springer, Berlin, 1987).
[52] *Handbook of Thermodynamic and Transport Properties of Alkali Metals* edited by R.W. Ohse (Blackwell, Oxford, 1985).
[53] J.-P. Hansen and G. Zerah, Phys. Lett. **108A**, 277 (1985); G. Zerah and J.-P. Hansen, J. Chem. Phys. **84**, 2336 (1986).
[54] G.A. Martynov, *Fundamental Theory of Liquids: Method of Distribution Functions* (Hilger, Bristol, 1992).
[55] R. Evans, D.C. Hoyle, and A.O. Parry, Phys. Rev. A **45**, 3823 (1992); R. Evans, R.J.F. Leote de Carvalho, J.R. Henderson, and D.C. Hoyle, J. Chem. Phys. **100**, 591 (1994); R. Evans and R.J.F. Leote de Carvalho (unpublished).
[56] G. Kahl and G. Pastore, J. Phys. A **24**, 2995 (1991).
[57] E. Kierlik and M.-L. Rosinberg, Phys. Rev. A **42**, 3382 (1990).
[58] S. Phan, E. Kierlik, M.-L. Rosinberg, B. Bildstein, and G. Kahl, Phys. Rev. E **48**, 618 (1993).
[59] Y. Rosenfeld, J. Chem. Phys. **89**, 4272 (1988).
[60] Y. Rosenfeld, D. Levesque, and J.-J. Weis, J. Chem. Phys. **92**, 6818 (1990).
[61] B. Bildstein and G. Kahl, Phys. Rev. E **47**, 1712 (1993); J. Chem. Phys. **100**, 5882 (1994).
[62] Y. Rosenfeld, *ACS Symposium Series No. 629,* edited by B. B. Laird, R. B. Ross, and T. Fiegler (ACS Publishing, Washington, 1996).
[63] Y. Rosenfeld, J. Stat. Phys. **37**, 215 (1984); **42**, 437 (1986).